Smart Nanoparticles for Protein Controlled Delivery

Joana Filipa Pereira de Brito
joanadebrito@tecnico.ulisboa.pt

Instituto Superior Técnico, Lisboa, Portugal

December 2021

Abstract

In the last years, increase interest have been paid to drug delivery systems, given a special attention to mesoporous silica nanoparticles (MSNs) due to their unique characteristics: high surface area and pore volume, tunable pore size, biocompatibility and easy surface modification. As cargo molecules, proteins are potent biotherapeutics that can be used in the treatment of several human diseases, as for example cancer and diabetes. Furthermore, have several advantages over conventional drugs, in which are included higher specificity, greater activity, and less toxicity. However, their low stability and large size pledge their therapeutic effects making a challenge their delivery into the target place and in a controlled manner. In this study, high pores mesoporous silica nanoparticles were synthesized for the controlled delivery of lysozyme by differently functionalize the nanoparticles. For this purpose, MSNs were functionalized with two different molecules N-(Trimethoxy silyl)propyl-N,N,N-trimethylammonium chloride (CAT) and trimethoxy(propyl)silane (PTES), and the remained were not functionalized. It was confirmed that, depending on the functionalization of the particles, the release kinetics was changed, being higher for MSN-CAT, lower for MSN-PTES and MSN-BARE. The release of lysozyme with dense silica nanoparticles (Stöber) was also performed, being verified that the release in MSNs occurs namely of molecules incorporated into the pores, since the initial kinetics of lysozyme release is much higher in Stöber. These results suggest that through different funcionalizations of the novel platform, we can control the release kinetics of the loaded protein.
Keywords: mesoporous silica nanoparticles, protein, functionalization, controlled delivery

1. Introduction

Proteins are large biomolecules which size goes from 1 to 100 nm , responsible for a diverse and essential functionalities in the biological organism, such as catalysing metabolic reactions, providing structure to cells and organisms, DNA replication, transportation of molecules from one location to another, defensive functions, regulatory functions, controlling cell fates, and maintaining the balance between cell survival and their death. [1, 2] Due to these reasons, proteins are called the "engines of life". [1] Besides their functions, proteins have some advantages over conventional drugs including a higher specificity (and then selectivity), greater activity, and lower toxicity [3]. In this sense, proteins are specific and potent biotherapeutics that can be of great use in the treatment of a variety of human diseases in which are included diabetes [2, 4], cancer [5, 3, 6, 7, 4], infections [4], inflammatory diseases [4], protein deficiency diseases [6], neurological disorders [2], cystic fibrosis [2], and others. Protein therapeutics comprise antibodies, cytokines, transcription factors and enzymes, among others [2].

Despite the great interest in protein delivery, the maintenance of their structural complexity, the susceptibility to enzymatic degradation and short circulation half-lives are some challenges that still need to be overcome.[8] These barriers can affect the effectiveness of delivery of many therapeutic proteins to the targeted disease sites. Therefore, to improve the effectiveness of protein therapeutics is required to overtake protein's challenges, and to achieve that goal is necessary to develop better protein delivery strategies or platforms [8].

One mechanism that can overcome many of these limitations and improving their offered therapy, is the development of a protein delivery strategy that can transport proteins and at the same time, have a controlled release at the target site. [3] Nowadays, there are many used protein delivery systems, although, the one that provides the tools and solutions to solve proteins delivery limitations is the employment of nanoparticles [2, 4]. Nanoparticles are very important vehicles not only because of their small size, typically in the range of 10 to 150 nm, but also because they are very promising in surpassing some of the limitations imposed by protein delivery.

Over the past years, Mesoporous Silica Nanoparticles (MSNs) have been considered the most promising drug delivery system due to their unique characteristics: high specific surface area; large pore volume; simple surface functionalization; and, great biocompatibility. [5, 9, 8] Their characteristics enable them to encapsulate a variety of therapeutic agents including pharmaceutical drugs, therapeutic proteins, and genes, delivering them into the desired location. [5] Therefore, MSNs have been seen as a vehicle that can overcome the disadvantages posed by traditional protein delivery systems.

However, there are still some challenges that need to be overcome, to make mesoporous silica nanoparticles a good protein delivery platform. One of them being to provide a controlled release of the protein in the desired locations. [8]

Aim of the work: The objective of this work is to develop a novel nanovehicle for protein controlled delivery based on the interactions between the functionalized and non-functionalized mesoporous silica nanoparticles with the lysozyme (protein). The synthesized nanoparticles must be lower 100 nm in size and with wide pores in order to incorporate the protein molecules. For the functionalization of MSNs it was used two compounds: N-(Trimethoxy silyl)propyl-N,N,N-trimethylammonium chloride (CAT), a cationic silane; and trimethoxy(propyl)silane (PTES), a hydrophobic silane. This new protein delivery system should be able to release the loaded protein in a controlled manner accordingly with the respective functionalization.

2. Materials and Methods

2.1. Materials

Cetyltrimethylammonium bromide (CTAB, ≥99%, Sigma), n-octane (+99%, ACROS Organics), ethanolamine (≥99%, Sigma), tetraethoxysilane (TEOS, ≥99%, Aldrich), absolute ethanol (EtOH, ≥99%, Fisher Chemical), N-(Trimethoxysilyl)propyl-N,N,N-trimethylammonium chloride (CAT, 50% in methanol, Gelest, USA), trimethoxy(propyl)silane (PTES, 97%, Aldrich, USA) were used as received. The dry toluene was refluxed over calcium hydride for 24 h and then distilled before use. Deuterium oxide (D_2O, 99.9% atom, Eurisotop), 1,3,5-trioxane (≥ 99.0%, Fluka), and sodium hydroxide (NaOH pellets, PanReac) were used as received. Disodium hydrogen phosphate (Na_2HPO_4, 99%, Riedel-de-Haën), sodium dihydrogen phosphate monohydrate ($NaH_2PO_4.H_2O$, 98%, Panreac) and sodium hydroxide (NaOH, 98%, Sigma-Aldrich) were used to prepare the phosphate buffer solutions (PBS, 0.1 M pH 7.4). Lysozyme (muramidase) from chicken egg white, designated by lysozyme for molecular biology (PanReac, Germany) was used as a model cargo for the release studies in a 2 mL eppendorf tube. Deionized water from a Millipore system Milli-Q ≥ 18 MΩ cm (with a Millipak membrane filter 0.22 μm) was used in the preparation of solutions and in synthesis.

2.2. Methods

2.2.1. Synthesis of Mesoporous Silica Nanoparticles (MSNs)

Mesoporous Silica Nanoparticles were synthesized following a method described by *Gustafsson et al.* [10]. In a polypropylene flask, were added CTAB (0.2 g), n-octane (19.9 g/24.8 mL), ethanolamine (18.6 μL) and deionized water (62 g). The mixture was left stirring for 1h, at a constant velocity of 600 rpm and 70 °C. Afterwards, TEOS (2 g) were added dropwise, and the solution was left stirring for 20h at the same velocity and temperature. The particles were recovered by centrifugation (90 000 rpm for 20 min), and the solid washed three times with pure ethanol. The nanoparticles obtained were dried at 60 °C in a ventilated oven overnight.

2.3. Template removal

The organic template of the synthesized nanoparticles was removed through calcination. The isothermal annealing of silica nanoparticles was performed for 6h under air atmosphere, at 1°C/min until it reached the 550°C, in a vertical tube furnace with glass reactor.

2.4. MSNs functionalization

The MSNs functionalization was performed using a cationic alkoxysilane, N-(Trimethoxy silyl)propyl-N,N,N-trimethylammonium chloride (CAT) or a hydrophobic alkoxysilane, trimethoxy(propyl)silane (PTES). For CAT functionalization, MSN (100 mg) was dispersed in a solution of dry toluene (5 mL) and CAT (50 μL), while for PTES functionalization, MSN (100 mg) was dispersed in a solution of dry toluene (5 mL) and PTES (45 μL). Both mixtures were kept at 125 °C with an argon atmosphere for 24h. The functionalized nanoparticles, MSN-CAT and MSN-PTES, were recovered by centrifugation (9 500 rpm for 10 minutes) and washed three times with ethanol. The solid was dried at 60 °C for 24h.

2.5. Loading and release of Lysozyme

To load the protein molecules into the pores of MSNs it was used the physical adsorption method. Lysozyme was used as a model protein molecule to test the load and release capability of the functionalized and non-functionalized nanoparticles, MSN-CAT, MSN-PTES and MSN. A phosphate buffer solution of lysozyme (100×10^{-6} M, 4 mL) was added to dry nanoparticles (20 mg), and the dispersion was left shaking for 115h at room temperature. The dispersion was divided in 3 eppedorf tubes (2 mL)

and centrifuged to remove the unloaded protein. The nanoparticles, of each eppendorf tube, were redispersed in phosphate buffer (0.5 mL, pH 7.4) and, afterwards, all volume was added into an eppendorf and centrifuged. The dispersion was redispersed in phosphate buffer (2 mL, pH 7.4) and centrifuged. After, the supernatant (1 mL) was removed and transferred to a fluorescence cuvette, measuring the initial lysozyme concentration. Later, the supernatant was replaced in the eppendorf and transferred to the rotary wheel, starting the release process (speed 3). The supernatants from post-loading were recovered and used to determine the loading efficiency, by fluorescence: 0.01371 mmol.g^{-1} for MSN-CAT, 0.01965 mmol.g^{-1} for MSN-PTES and 0.01968 mmol.g^{-1} for MSN. The released lysozyme from the nanoparticles was also monitored through lysozyme fluorescence intensity from taken supernatants (1 mL) during the release process.

2.6. Characterization Methods

2.6.1. Transmission Electronic Microscopy (TEM)

TEM images were obtained on a Hitachi transmission electron microscope (Hitachi High–technologies, Tokyo, Japan), model H-8100, with a LaB_6 filament (Hitachi High-Technologies Europe GmbH, Krefeld, Germany) complemented with an accelerator voltage of 200 kV and a current of 20 μA. The microscope has incorporated a KeenView camera (Soft Imaging System, Münster, Germany) which through iTEM software allows the capture of TEM images. MSNs were dispersed in ethanol and dried on a Formvar carbon-coated copper grid 200 mesh (Ted Pella, Redding, CA, USA). TEM images were analyzed through Image J software, where the nanoparticles size/dimension, sphericity, polydispersity and morphology were estimated.

2.6.2. Nitrogen Adsorption-Desorption

The N_2 adsorption–desorption isotherms were obtained at 77 K (temperature of liquid nitrogen) for the degassed samples in a gas porosimeter with an accelerated surface area and porosimetry system (Micromeritics, model ASAP 2010, Norcross, GA, USA).

2.6.3. Proton Nuclear Magnetic Resonance (^{1}H NMR)

The ^{1}H NMR analysis was performed in a Bruker Avance III 400 spectrometer (Bruker BioSpin GmbH, Rheinstetten, Germany) operating at 400 MHz. Two solutions were prepared, a NaOH solution where 1 pellet was added to 6 mL of D_2O, and a 1,3,5-trioxane (used as internal standard, IS) solution of concentration 31 $\times$ 10^{-3} M in D_2O. In a NMR tube MSNs (5 mg), NaOH solution (400 μL) and 1,3,5-trioxane solution (100 μL) were added. The tube was sonicated until a clear solution was obtained.

2.6.4. Zeta-Potential

The Zetasizer Nano ZS (Malvern Instruments, model ZEN3600 UK) was used to performe the measurements. Zeta potentials were calculated from electrophoretic mobility using the Smoluchowski relationship. Disposable folded capillary cells (DTS1070) (Malvern Instruments, Worcestershire, UK) were used for the measurement of the zeta potentials, in which, each measurement was performed in triplicate.

2.6.5. Fluorescence Measurements

All measurements were performed in Horiba-JobinYvon (Kyoto, Japan) Fluorolog-3 spectrofluorimeter, using a fluorescent cell. The right angle geometry mode was used in all measurements (λ_{exc} = 280 nm, λ_{em} = 338 nm).

2.6.6. UV-Vis Spectroscopy

UV-660 UV-VIS Spectrophotometer (JASCO International, Tokyo, Japan), supplied with a double monochromator and photomultiplier tube detector for higher resolution. All the measures were carried out in same quartz cells as the fluorescence spectroscopy at room temperature

3. Results and Discussion

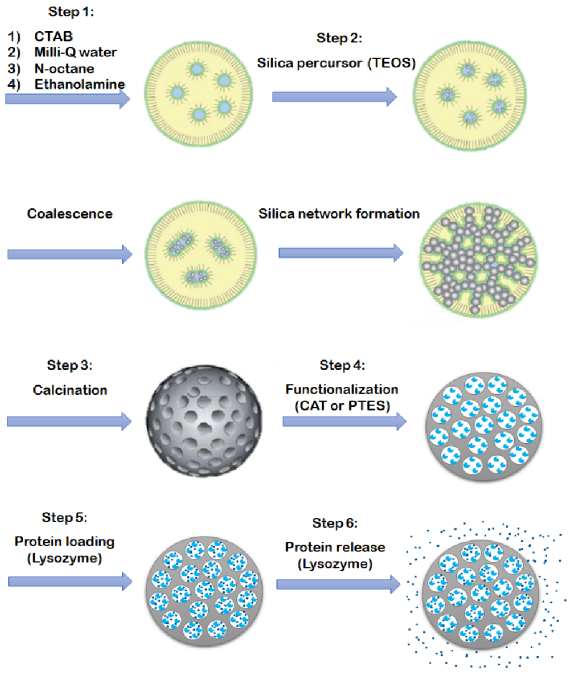

Figure 1: Scheme of the process carried out in this work: MSNs synthesis, functionalization, protein loading and protein release.

Our strategy to developing smart nanoparticles for the controlled delivery of proteins relies on the easy modification of mesoporous silica nanoparticles' surface. Therefore, after the template removal, they were functionalized with different silane compounds, which, depending on the interaction with the loaded cargo cause their release with different kinetics (figure 1).

3.1. MSNs synthesis and characterization

The MSNs were synthesized using an oil-in-water method [10], where three synthesis were performed under the same conditions, MSN_A, MSN_B and MSN_C. In order to determine MSNs' diameters, TEM images were taken in which 60 nanopaticles were analyzed. The obtained nanoparticles, have mean diameters of (71 ± 4) nm, (71 ± 8) nm and (70 ± 5) nm, for synthesis A, B and C respectively. In this way, the average diameter achieved through this synthesis method was (71 ± 6) nm, which is in line with the intended results. The nanoparticles also present a well-defined pore structure showing a snowflake morphology, which was preserved after calcination (figure 2).

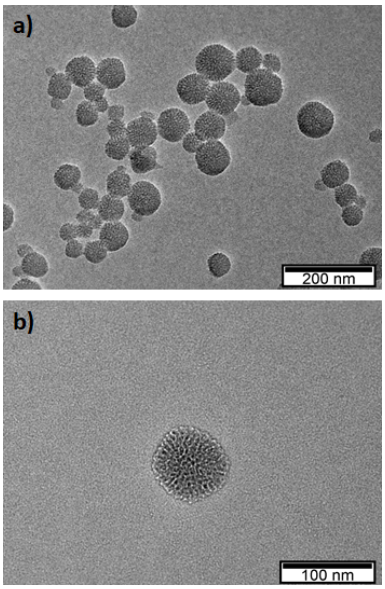

Figure 2: TEM images of MSN_C synthesis before, a), and after calcination, b), where it is visible their pore structure and morphology.

By analysing the images taken from TEM, was also possible to measure their sphericity (S), how circular the synthesised nanoparticles are. A value closest to unity indicates the highest circularity of the particles, in this way, MSNs with values farther from the unit are non-spherical. The obtained values on this parameter for the three samples were (1.066 ± 0.003), (1.067 ± 0.005) and (1.085 ± 0.005), for synthesis A, B and C, respectively. Regarding these values, since they are very close to the unity we can conclude that the synthesised particles have a spherical shape.

With the nitrogen adsorption study (figure 3) it was observed a typical isotherm of mesoporous materials (Type IV). From the BET analysis, the specific surface area was determined, 1260 (m^2/g), and using the Barrett–Joyner–Halenda (BJH) method it was obtained a pore volume of 1.1 mL/g with a pore diameter of 6 nm.

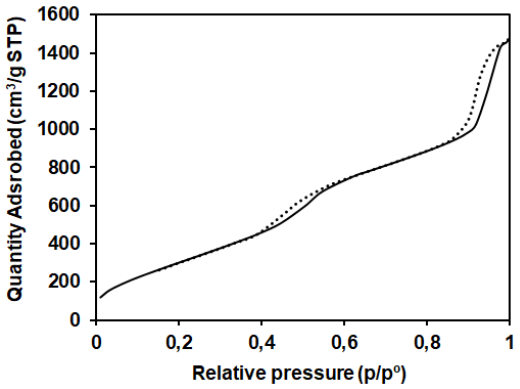

Figure 3: Nitrogen adsorption-desorption isotherms for MSN_C and corresponding size distribution.

Hence, the process of synthesis of MSNs by water-in-oil emulsions is a very well reproducible process, where, the particles have been successfully synthesized, by having all the desired characteristics: high surface area, large pore width and diameter lower than 100 nm.

3.2. MSNs functionalization

Following the synthesis and template removal of the mesoporous silica nanoparticles, the next step was to modify their pore surface. The surface of the nanoparticles was modified with two compounds: CAT (a cationic silane), and PTES (an hydrophobic silane). After their modification, three differently functionalized particles were obtained: MSN-CAT which has positive charges, MSN-PTES hydrophilically functionalized, and, MSN-BARE without any functionalization, therefore fully negatively charged because of the silica. The nanoparticles were recovered by centrifugation and washed three times with ethanol to remove the compound not bonded to the particle's surface.

The success of the previous steps was confirmed by zeta-potential measurements, which indicates a change in the nanoparticles' external charge upon the immobilization of the molecules. With this measurements were obtained an average surface charge of (29 ± 6) mV, (-21 ± 4) mV and (-34 ± 4) mV, for MSN-CAT, MSN-PTES and MSN-BARE, respectively. The nanoparticle's zeta-potential is

different according to the respective functionalization, being positive for CAT-functionalized MSNs and negative for PTES-functionalized MSNs and non-functionalized MSNs. Hence, the MSN-BARE show the most negative potential because the silanol groups have their isoelectric point at pH 2, so above this value the nanoparticles have a negative charge. The MSN-CAT exhibit positive potentials due to the presence of the quaternary amine function which shifts the isoelectric point to higher pH values. Additionally, for MSN-BARE, it is shown a lower negative potential comparatively to the bare nanoparticles, due to the presence of hydrophobic molecules on its surface. The modifications made on the surface of the nanoparticles were thus successful.

To quantify the molecules linked to the particles, it was used the technique ^{1}H NMR as described by Crucho *et al.* [11]. In their method, the silica matrix is first destroyed with a concentrated solution of NaOH, and then an internal standard (trioxane) is used in the quantification. The ^{1}H NMR spectra of the functionalized nanoparticles is presented in figure 4, where A is for MSN-CAT and B for MSN-PTES. The peaks d) in figure 4 A and c) in figure 4 B were used to estimate the number of organic molecules grafted onto the surface of MSNs, through the comparison with the trioxane integrated intensity.

Through ^{1}H NMR, it was determined the CAT concentration at the MSN surface, being 0.38 mmol/g_{MSN}, corresponding to a surface density of 0.18 molecules/nm^2 (table 1). The same was done to determine the PTES concentration at the nanoparticles surface, being 0.33 mmol/g_{MSN}, and corresponding to a surface density of 0.16 molecules/nm^2 (table 1).

Table 1: Functional groups quantification by ^{1}H NMR

Measured properties	MSN-CAT	MSN-PTES
[PTES or CAT] (mmol/g_{MSN})	0.38	0.33
Surface coverage (molecules/nm^2)	0.18	0.16

Analyzing the quantification obtained for each MSN, it is possible to observe that both concentration of the functionalizing molecule per gram of nanoparticle and surface coverage are very similar for the two samples. This means that the functionalization is very effective regardless the type of compound, which is what was expected.

3.3. Loading and release study

The proof of concept for these MSNs as protein controlled delivery nanocarriers was made through the release of lysozyme (Lyz), which 3D structure is present in figure 5. The lysozyme protein was selected due to its fluorescence properties since in its constitution it has 6 tryptophans [15, 16]. In addition, it has a lower size than the pore width of the synthesized nanoparticles, having an elliptical conformation of size 4.5 nm×3.0 nm×3.0 nm.

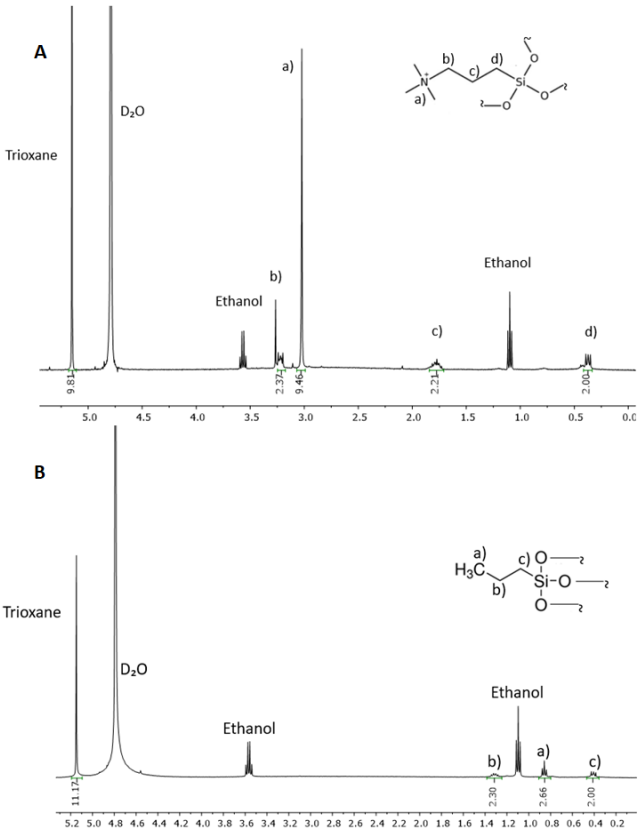

Figure 4: ^{1}H NMR spectrum in D_2O of MSN-CAT (A) and MSN-PTES (B). In MSN-CAT, a) correspond to CH_3 protons of N-trimethoxysilylpropyl-N,N,N-trimethylammonium chloride and b), c) and d) correspond to CH_2 protons. [12] In MSN-PTES, a) correspond to CH_3 protons of trimethoxy(propyl)silane and b) and c) correspond to CH_2 protons. [13, 14]

Lysozyme is a single polypeptide chain of 129 amino acids, with a molecular weight of 14.3 kDa and four dissulfide bridges in its constitution. One important characteristic of this protein, is that it is strongly basic, with an isoelectric point at pH 10.7. [17, 18, 19, 20, 21, 22, 23, 24] Another important feature is its capability of lyzing bacteria through the hydrolyzation of specific peptidoglycan linkages in the cell wall. Therefore, it has very important functions in the human body, such as boosting the immune system, antiviral activities, potentiality as an anticancer agent (since inhibits the tumor formation and growth), improvement of the efficiency of chemotherapy treatments, among others. [23]

Figure 5: Lysozyme 3D structure (adapted from [25]).

3.3.1. Lysozyme incorporation

The main advantage of using mesoporous silica nanoparticles as nanovehicles in the delivery application is the large cargo amount that they can carry due to their high surface area and pore volume. Additionally, through the functionalization of the nanoparticle's surface it is possible to adjust the amount of cargo molecules that can be carried until it reaches the desired location.

It is important to bear in mind that in this work the cargo molecule is from biological origin. Thus, the method of incorporation to be used must remain intact the biological activity of the protein. Taking this into consideration, the employed method to load the lysozyme into MSNs was physical adsorption from an aqueous solution into the mesopores [26, 27].

To quantify lysozyme incorporation and release, several lysozyme solutions were prepared in PBS at pH 7.4 and their absorption and emission spectres were determined. With the absorption study, it was determined the wavelength at which occurs the lysozyme absorption maximum, $\lambda = 277$ nm. Therefore, it was used the wavelength of 280 nm, to perform the emission spectra of lysozyme, and determined the wavelength at which occurs the lysozyme maximum of emission, $\lambda = 338$ nm. [28, 29, 30, 31] Afterwards, a calibration curve was made for this wavelength, and a linear fit from the experimental points gave the following regression equation: $\mathrm{Em}_{max} = (7.5 \pm 0.4) \times 10^6$ c - $(3.2 \pm 2.2) \times 10^6$, where c is the concentration of lysozyme solution in μM.

After performing the loading process, the excess of lysozyme was removed by centrifugation and the supernatants used to quantify the protein that was not loaded. With this purpose, the supernatants were analysed by fluorescence spectroscopy and the emission spectra recorded. Using the calibration curve, the concentration and the molar amount of lysozyme that was not incorporated were determined, and, consequently, the amount of protein incorporated into the MSNs was determined. As a control it was used a lysozyme solution of 10 μM, in order to later normalize all the data to be comparable.

The obtained amount of incorporated lysozyme was 69%, 98% and 98%, for MSN-CAT, MSN-PTES and MSN-BARE, respectively. The results obtained are in line with our expectations since: (1) for the interaction of MSN-CAT with the protein, the nanoparticles have positive charges on their surface that repel the lysozyme. Despite the electrostatic repulsion interaction between them, a high percentage of incorporation is still obtained, 69%, which may be due to the hydrophobic interactions between the hydrophobic part of the silane compound and the hydrophobic part of the protein. The protein also contains hydrophilic parts, however, due to its large size the hydrophobic part may have a greater influence than the hydrophilic one, thus leading to a lower percentage of incorporation compared to the others MSNs, about 30% smaller; (2) for the interaction of MSN-BARE with lysozyme, the interactions are only electrostatic, and, as such the negatively charged silica will adsorb the positively charged lysozyme reaching a very high incorporation percentage, 98%; and, lastly, (3) for the interaction of MSN-PTES with lysozyme, the interactions are mainly due to the ability of silica interact with the protein via electrostatic interactions, but also of PTES interact with lysozyme via hydrophobic interactions [32].

We can conclude that by functionalizing differently the MSNs we can control the amount of cargo molecules incorporated into the nanoparticles.

3.3.2. Lysozyme release

The release of lysozyme was followed for about 43 days, where each day 1 mL of the supernatants of each particle formation were removed and replaced by 1 mL of PBS. To monitor the release of lysozyme from the nanoparticles we used fluorescence cuvettes, where the respective supernatant of each particle formation as well as the lysozyme control solution (c = 10 μM) were placed. In figure 6 we represent an example of the emission spectra of each sample, measured at day 8 of the release study.

To determine the quantity of lysozyme that was released in each supernatant, the value of the measured emission spectrum corresponding to the wavelength of 338 nm, was selected and replaced in the calibration curve equation.

On the image A of figure 7, we represent the number of moles of lysozyme released over the 43 days for the different nanoparticles formations, while on image B of the same figure, we represent the quantity of lysozyme released for the first 13 days of the experiment. Analyzing these graphics, it is possi-

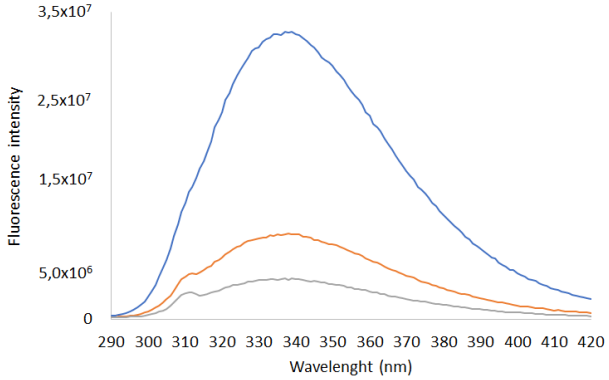

Figure 6: Example of a measured emission spectrums of each sample at day 8, during the release study. Blue line - represents the spectrum for nanoparticles MSN-CAT; Orange line - represents the spectrum for nanoparticles MSN-PTES; Grey line - represents the spectrum for nanoparticles without functionalization, MSN-BARE.

ble to see that the release kinetics for MSN-CAT is very fast at the beginning but it decreases over time, where in the last days of release it seems to be almost reaching a plateau, where there is no longer release of the loaded cargo. On the contrary, for MSN-PTES and MSN-BARE, we have two different release regimens. In the first one (5 days), the lysozyme release is very slow or almost null while in the second one, a larger release of lysozyme is observed.

The data obtained from the release study of lysozyme is presented in table 2. During the first 13 days of release, MSN-CAT releases about 36% of the incorporated Lyz while MSN-PTES and MSN-BARE release only 7% and 5%, respectively. This means that in the first 13 days of the experiment, MSN-PTES and MSN-BARE have a more controllable release than MSN-CAT.

Table 2: Released lysozyme percentage for the different nanoparticle's formation, for the first 13 days and the full 43 days of release.

Samples	Released (%)
$MSN\text{-}CAT_{13}$	36
MSN-CAT	64
$MSN\text{-}PTES_{13}$	7
MSN-PTES	32
$MSN\text{-}BARE_{13}$	5
MSN-BARE	26

Comparing the values obtained on the 13th day

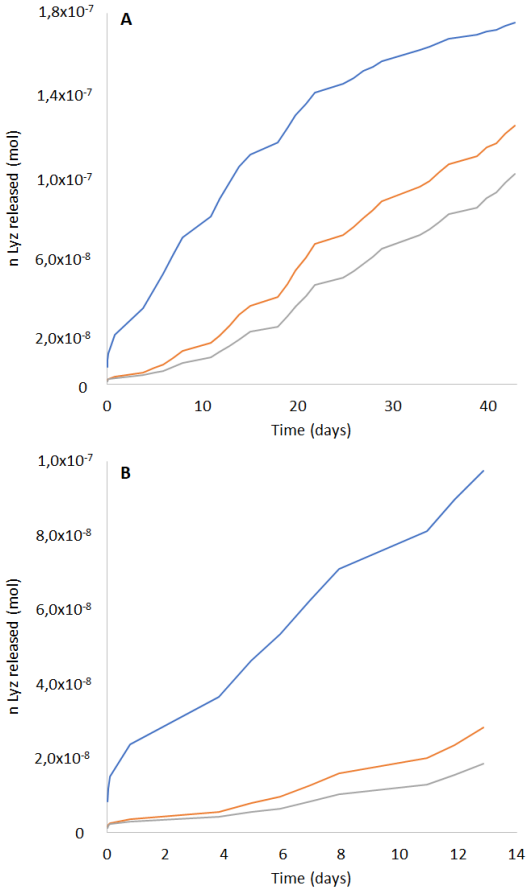

Figure 7: Released number of moles of lysozyme throughout the 43 days (A) and for the first 13 days of release (B), for each formation of nanoparticles. Blue line - represents the released Lyz for the nanoparticles MSN-CAT; Orange line - represents the released Lyz for the nanoparticles MSN-PTES; Grey line - represents the released Lyz for the nanoparticles without functionalization, MSN-BARE.

with those obtained on the 43rd day, it is also possible to verify that MSN-CAT released 56% of the total protein. Thus, the release kinetics from the 13 days is faster than the release kinetics for the rest of the study. In contrast, MSN-PTES and MSN-BARE released 23% and 18% of the amount of Lyz released at the end of 43 days. Hence, initially these nanoparticles have a more controlled release, where from day 13 onwards, the particles have higher release, but with an approximately constant kinetics.

Overall, a higher percentage of released Lyz was achieved for MSN-CAT, 64%, while for MSN-PTES and MSN-BARE lower released percentages were achieved, 32% and 26%, respectively. The results obtained are in agreement with expectations due to the same reasons already mentioned for the percentages of incorporation for each MSN. Regard-

ing MSN-PTES and MSN-BARE nanoparticles, it is still possible to verify that they have similar release kinetics, however, the higher release occurs for MSN-PTES. This happens, due to the fact that hydrophobic interactions are weaker than electrostatic ones and, as such, MSN-PTES release a little more protein than MSN-BARE (which only have electrostatic interactions with the protein).

With this analysis, we can conclude that the release of lysozyme is strongly dependent on the functionalization of the MSNs. Thus, depending on the functionalization used, it is possible to control protein delivery.

3.3.3. MSN vs. Stober

To determine if lysozyme was actually incorporated into the pores of the nanoparticles or if it was just adsorbed on its surface, we also studied the release from Stöber silica nanoparticles, which are dense silica nanoparticles (without pores).

We used an amount of Stöber nanoparticles with approximately the same total surface area than MSNs. The mass of Stöber particles to use in the incorporation was determined, so that the total surface area was the same in both experiments. The calculations are presented in table 3.

Table 3: Data calculated to obtain the mass of Stöber silica nanoparticles to use in the release process, knowing the density of each nanoparticle.

Parameters	MSN	Stöber
Diameter (nm)	70	80
Density (g/mL)	0.4	1.6
V_p (nm^3)	179 594.38	268 082.57
V_{total} (mL)	0.05	0.057
A_p (nm^2)	15393.80	20106.19
A_{total} (nm^2)	4.2857×10^{18}	4.2857×10^{18}
$Mass_p$ (mg)	7.1838×10^{-14}	4.2893×10^{-13}
$Mass_{total}$ (mg)	20	91.43
N_p	2.7804×10^{14}	2.1315×10^{14}

The presented parameters are: diameter (nm) - diameter of each particle; density (g/mL) - density of each particle; V_p - volume of one particle; V_{total} - total volume occupied by the number of particles used; A_p - surface area of one particle; A_{total} - total surface area obtained with the number of particles used; $Mass_p$ - mass per one particle; $Mass_{total}$ - total mass of nanoparticles used in the study; and, N_p - number of nanoparticles used in the study.

In order to compare the release study of Stöber nanoparticles with MSN-BARE, the protein incorporation and release was carried out under the same conditions. Figure 8 shows the first 4 days of release of Stöber silica nanoparticles and MSN-BARE.

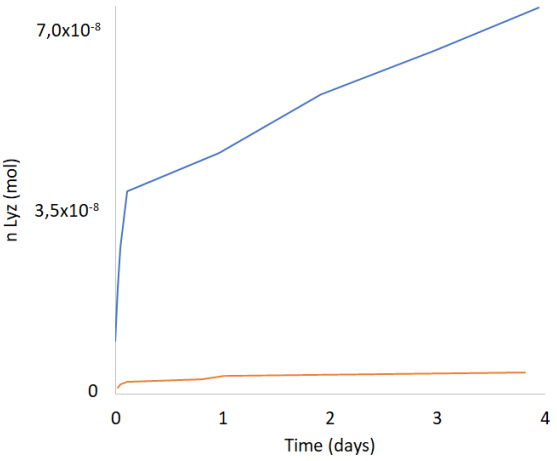

Figure 8: Released number of moles of lysozyme throughout the first 4 days of release, for Stöber silica nanoparticles and MSN-BARE. Blue line - represents the released quantity of Lyz for the Stöber nanoparticles; Orange line - represents the released quantity of Lyz for the nanoparticles MSN-BARE.

As we can observe, the initial release kinetics is very high for Stöber nanoparticles while for MSN-BARE is only residual. Which means that the protein is all adsorbed on the Stöber nanoparticles surface, leading to a faster release of lysozyme, while for MSN-BARE, due to the existence of pores, these protect the protein, and almost none of the protein is released.

4. Conclusions

In this work, a novel nanovehicle for protein controlled delivery based on the interactions between the functionalized MSN pore walls and the cargo protein was prepared. Nanoparticles with lower size and high pore volumes and width were successfully synthesized by an emulsion-based method.

After template removal, the nanoparticle's surface was modified with two functional groups: N-trimethoxysilylpropyl- N, N, N - trimethylammonium chloride (CAT) and trimethoxy(propyl) silane (PTES). It was achieved a very similar surface coverage for both functionalized nanoparticles, MSN-CAT and MSN-PTES, which means that the functionalization was very effective. However, since the synthesized nanoparticles have a very high surface area, to obtain a higher surface coverage, a higher concentration of functionalizing molecules should be used.

The proof of concept for these functionalized MSNs in protein controlled delivery was made through the release study of lysozyme, where different interactions between the MSNs and the protein

were studied: MSN-CAT, the nanoparticles functionalizes with the cationic substance, a cationic-cationic interaction with Lyz was studied; MSN-PTES, the nanoparticles functionalized with the hydrophobic compound, a hydrophobic-hydrophobic interaction with Lyz was studied; and, MSN-BARE, without any functionalization, an anionic-cationic interaction with Lyz was studied.

The protein released studies demonstrate a strong relationship between the nanoparticle functionalization and the protein release kinetics. MSN-CAT have a high initial release kinetics that decreases overtime, while the contrary occurs for MSN-PTES and MSN-BARE. It is important to emphasize that MSN-PTES have a slightly higher release kinetics than MSN-BARE due to the breakdown of hydrophobic interactions between the PTES compound and proteins. Thus, we can conclude that among the three nanoparticles formation, those that have a more controlled delivery of lysozyme are MSN-PTES and MSN-BARE. Also, the comparison release study between MSN-BARE and Stöber nanoparticles allowed to conclude that the protein molecules are incorporated inside the pores.

Overall, this novel platform proved that by functionalizing differently the mesoporous silica nanoparticles creates a system where the release kinetics of the loaded protein can be controlled. In this way, opens excellent prospects for the controlled delivery of proteins, with possible therapeutic applications.

References

[1] Suryani Saallah and I. Wuled Lenggoro. Nanoparticles Carrying Biological Molecules: Recent Advances and Applications. *KONA*, 35(0):89–111, 2018.

[2] María Rocío Villegas, Alejandro Baeza, and María Vallet-Regí. Nanotechnological Strategies for Protein Delivery. *Molecules*, 23(5):1008, April 2018.

[3] Ravi Vaishya, Varun Khurana, Sulabh Patel, and Ashim K Mitra. Long-term delivery of protein therapeutics. *Expert Opinion on Drug Delivery*, 12(3):415–440, March 2015.

[4] Mikyung Yu, Jun Wu, Jinjun Shi, and Omid C. Farokhzad. Nanotechnology for protein delivery: Overview and perspectives. *Journal of Controlled Release*, 240:24–37, October 2016.

[5] Fangqiong Tang, Linlin Li, and Dong Chen. Mesoporous Silica Nanoparticles: Synthesis, Biocompatibility and Drug Delivery. *Adv. Mater.*, 24(12):1504–1534, March 2012.

[6] Ming Yan, Juanjuan Du, Zhen Gu, Min Liang, Yufang Hu, Wenjun Zhang, Saul Priceman, Lily Wu, Z. Hong Zhou, Zheng Liu, Tatiana Segura, Yi Tang, and Yunfeng Lu. A novel intracellular protein delivery platform based on single-protein nanocapsules. *Nature Nanotech*, 5(1):48–53, January 2010.

[7] Anne Yau, Jinhyung Lee, and Yupeng Chen. Nanomaterials for Protein Delivery in Anticancer Applications. *Pharmaceutics*, 13(2):155, January 2021.

[8] Hai-Jun Liu and Peisheng Xu. Smart Mesoporous Silica Nanoparticles for Protein Delivery. *Nanomaterials*, 9(4):511, April 2019.

[9] Miguel Manzano and María Vallet-Regí. Mesoporous Silica Nanoparticles for Drug Delivery. *Adv. Funct. Mater.*, 30(2):1902634, January 2020.

[10] Hanna Gustafsson, Simon Isaksson, Annika Altskär, and Krister Holmberg. Mesoporous silica nanoparticles with controllable morphology prepared from oil-in-water emulsions. *Journal of Colloid and Interface Science*, 467:253–260, April 2016.

[11] Carina I. C. Crucho, Carlos Baleizão, and José Paulo S. Farinha. Functional Group Coverage and Conversion Quantification in Nanostructured Silica by ^{1} H NMR. *Anal. Chem.*, 89(1):681–687, January 2017.

[12] Fisher Scientific. N-[3-(Trimethoxysilyl)propyl]-N,N,N-trimethylammonium chloride, 50% in methanol, Thermo Scientific™ | Fisher Scientific.

[13] Ltd.(APAC) Tokyo Chemical Industry Co. Trimethoxy(propyl)silane.

[14] Merck. Trimethoxy(propyl)silane 97 1067-25-0.

[15] UniProt. Protein Structure and Function, July 1986.

[16] YANG Hui, XIAO Xue, ZHAO Xuesong, and WU Yan. Intrinsic Fluorescence Spectra of Tryptophan, Tyrosine and Phenyloalanine. page 10, 2015.

[17] Clem Maidment, Allan Dyson, and Jennifer Beard. A study into measuring the antibacterial activity of lysozyme-containing foods. *Nutrition & Food Science*, 39(1):29–35, February 2009.

[18] bioseutica. LYSOZYME | Bioseutica®.

[19] Kai Zheng, Miao Lu, Yufang Liu, Qiang Chen, Nicola Taccardi, Norbert Hüser, and Aldo R Boccaccini. Monodispersed lysozyme-functionalized bioactive glass nanoparticles with antibacterial and anticancer activities. *Biomed. Mater.*, 11(3):035012, June 2016.

[20] Jeanette Held and Sander van Smaalen. The active site of hen egg-white lysozyme: flexibility and chemical bonding. *Acta Crystallogr D Biol Crystallogr*, 70(4):1136–1146, April 2014.

[21] Gao Gao and Ping Yao. Structure and activity transition of lysozyme on interacting with and releasing from polyelectrolyte with different hydrophobicity. *J. Polym. Sci. A Polym. Chem.*, 46(14):4681–4690, July 2008.

[22] Soohwan Yum, Moon Jong Kim, Yongbin Xu, Xiao Ling Jin, Hee Young Yoo, Ji-Won Park, Ji Hee Gong, Kwang-Min Choe, Bok Luel Lee, and Nam-Chul Ha. Structural basis for the recognition of lysozyme by MliC, a periplasmic lysozyme inhibitor in Gram-negative bacteria. *Biochemical and Biophysical Research Communications*, 378(2):244–248, January 2009.

[23] Jennifer Kovacs-Nolan, Marshall Phillips, and Yoshinori Mine. Advances in the Value of Eggs and Egg Components for Human Health. *J. Agric. Food Chem.*, 53(22):8421–8431, November 2005.

[24] J. Ross Colvin. THE SIZE AND SHAPE OF LYSOZYME. *Can. J. Chem.*, 30(11):831–834, November 1952.

[25] D.R. Holland and P. Shih. RCSB PDB - 1LSM: THERMAL STABILITY DETERMINANTS OF CHICKEN EGG-WHITE LYSOZYME CORE MUTANTS: HYDROPHOBICITY, PACKING VOLUME AND CONSERVED BURIED WATER MOLECULES, November 1994.

[26] Jessica M. Rosenholm, Cecilia Sahlgren, and Mika Linden. Multifunctional Mesoporous Silica Nanoparticles for Combined Therapeutic, Diagnostic and Targeted Action in Cancer Treatment. *CDT*, 12(8):1166–1186, July 2011.

[27] Montserrat Colilla, Blanca González, and María Vallet-Regí. Mesoporous silicananoparticles for the design of smart delivery nanodevices. *Biomater. Sci.*, 1(2):114–134, 2013.

[28] Yangang Wang, Jiawen Ren, Xiaohui Liu, Yanqin Wang, Yun Guo, Yanglong Guo, and Guanzhong Lu. Facile synthesis of ordered magnetic mesoporous -Fe2O3/SiO2 nanocomposites with diverse mesostructures. *Journal of Colloid and Interface Science*, 326(1):158–165, October 2008.

[29] Jianxiong Xu, Weiwei Liu, Yunfei Yu, Jingjing Du, Na Li, and Lijian Xu. Synthesis of mono-dispersed mesoporous SBA-1 nanoparticles with tunable pore size and their application in lysozyme immobilization. *RSC Adv.*, 4(71):37470–37478, 2014.

[30] Xu Yang, Shi-Jun Liao, Zhen-Xing Liang, Yue-Xia Li, and Li Du. Gelatin-assisted templating route to synthesize sponge-like mesoporous silica with bimodal porosity and lysozyme adsorption behavior. *Microporous and Mesoporous Materials*, 143(2-3):263–269, September 2011.

[31] Mani S. Bhattacharyya, Pradip Hiwale, Monica Piras, Luca Medda, Daniela Steri, Marco Piludu, Andrea Salis, and Maura Monduzzi. Lysozyme Adsorption and Release from Ordered Mesoporous Materials. *J. Phys. Chem. C*, 114(47):19928–19934, December 2010.

[32] Oriana Osta, Marianne Bombled, David Partouche, Florian Gallier, Nadège Lubin-Germain, Nancy Brodie-Linder, and Christiane Alba-Simionesco. Direct Synthesis of Mesoporous Organosilica and Proof-of-Concept Applications in Lysozyme Adsorption and Supported Catalysis. *ACS Omega*, 5(30):18842–18848, August 2020.